Proceedings of the 26th International Conference on
Port and Ocean Engineering under Arctic Conditions
June 14-18, 2021, Moscow, Russia

Thermal deformations of frozen soils at the design of hydrotechnical structures in the Arctic region

Artem Nesterov[1], Aleksey Marchenko[2], Nicolai Vasiliev[3]
[1] Peter the Great Saint-Petersburg Polytechnic University, Saint-Petersburg, Russia
[2] The University Centre in Svalbard (UNIS), Longyearbyen, Norway
[3] JSC "Vedeneev VNIIG", Saint-Petersburg, Russia

ABSTRACT

Permafrost complicates the development of new oil and gas fields and capacity increase of such year-round cargo turnover as the Northern Sea Route, which is a part of the Strategy for the Development of Sea Port Infrastructure until 2030 in the Russian Federation and in the other Arctic regions. The relevance of this paper lies in the area of determination of seasonal deformations of frozen ground as part of the design of hydrotechnical structures (Sabetta seaport, Utrenniy LNG terminal, etc) to ensure continuous transport communication of the Arctic regions. In 2016-2019, a number of experiments was carried out at the university center on Svalbard in order to determine the deformations of artificially frozen soils with different water and particles content. The experiments were carried out in cold camera, where the temperature varied from -5 to -20 ºC. The deformation values and coefficients of thermal expansion obtained with the use of fiber-optic Bragg grating sensors and thermistor strings can be used in the calculations of the considering structures.

KEY WORDS: Permafrost, Hydrotechnical Structures; Arctic Region; Frost Heave; Fiber-Optic Sensors.

INTRODUCTION

The development of the Arctic regions is directly related to the intensive expansion of port infrastructure. For example, in the Russian Federation, an appropriate Development Strategy was adopted up to 2030. The specific harsh climatic conditions of the Arctic affect the design processes of structures, including hydrotechnical facilities which have foundations with permafrost (Alhimenko A.I., et. al., 2003). Currently, there is still a problem of the characteristics monitoring during operation and determination of the soil exact parameters at the calculations stage of such structures due to phase transformations within seasonal thawing / freezing processes (Andersland O. B. and Ladanyi B., 2003).

Initially, much attention was paid to the problems of frost heave, but the problems associated with the behavior of frozen soils under cyclic changes of negative temperatures are also important due to the presence of unfrozen water in frozen soils (Grechishchev, et al., 1983). The phase transformations influence thermal deformations of frozen soils (Ershov, 1990). Compressive or tensile deformations arising in the soils under the action of the air temperature changes influence the formations of frost cracks passing through the active soil layer into permafrost (Chzhan, Velikin, 2014). It may create deformation and destruction of engineering structures.

Ice cementation of mineral particles in frozen soils is of primary importance for assessing of their mechanical properties estimated by the ice content and the quantitative content of unfrozen pore water at a given negative temperature (Cheverev, 2004). At the same time, the construction of hydraulic structures inthe Arctic is affected by both sea water (such seaports as Sabetta, Tiksi, etc) and fresh water (such ports as Dudinka, Murmansk, etc). Therefore, in this work, a new technique for experimental studies of temperature deformations of frozen soils saturated with water of various salinity is proposed and implemented. Knowledge of the processes of thermal expansion of such soils is necessary for the design of berthing and soil structures the Arctic regions (Marchenko, Nesterov, Vasiliev, et. al., 2020). This paper is a continuation of the authors' work on the topic of temperature transformations of frozen soils in relation to their impact on hydrotechnical structures (Nesterov, et. al., 2020).

MATERIALS AND METHODS

The team Fiber Bragg Grating sensor (FBG) is a periodic grid with 40,000 cells burned by two laser beams inside the fiber with diameter of 9 μm. The grid length is 1 cm. Each FBG sensor reflect the light signal of a certain wavelength, depending on the grid characteristics, tension and temperature of the fiber. The incoming light signal is generated in the optical fiber by the source LED in the spectral range 1,500 ~ 1,600 nm. The wavelengths reflected by the FBG sensors are registered and analyzed by a spectrometer. To register changes inside a calibration device, a constant temperature is maintained in one of the sensors. The spectrometer, calibrator, and analyzer of the incoming optical signals are combined in one unit with four channels designed and manufactured in the company Advance Optic Solutions GmbH (Dresden). Every channel of the unit can transfer information from 16 FBG sensors embedded in the same fiber (Marchenko, Lishman, Wrangborg, et al., 2016).

FBG thermistor string and strain sensor are shown in Figure 1. Fiber cable with FBG temperature sensor is protected from mechanical deformations by thin metal tube of 1 mm diameter. The FBG thermistor string includes 12 FBG sensors embedded in the same fiber with 1 cm distance between neighbor sensors. The FBG thermistor string is protected from mechanical deformations by thin metal tube of 1 mm diameter and 25 cm length. The thermistor string is welded with optical fiber protected by blue plastic. The accuracy of temperature measuring, and nominal resolution is correspondingly equal to 0.4°C and 0.08°C. Strain sensor is embedded in the middle part of the fiber protected by transparent plastic with working length about 20 cm. The fiber inside transparent plastic is going through the screw and welded to fiber cable protected by yellow plastic. The strain sensor is mounted on a sample and pretended using two screws and bolts. The resolution of the strain sensors is 10^{-6}, and the accuracy is 5×10^{-6}.

The change of the wavelength (Δλ) of the light reflected by the Bragg grating is proportional to the fiber extension (ΔL/L) and the change of the fiber temperature (ΔT):

$$\Delta\lambda/\lambda = GF * \Delta L/L + TK * \Delta T \quad (1)$$

where GF = 0.719, "calibration factor"; TK = 5.5×10^{-6}, “thermal elongation factor”; L is the reference length of the fiber; λ is the reference length of the light reflected by the Bragg grating. The value of Δλ is measured by the spectrometer. From Equation 1 it follows that temperature changes of the fiber T should be known for the calculation of the fiber strain □L/L. In the experiment, the temperature of the strain sensor was measured by the FBG temperature sensor. The FBG thermistor string was installed to measure temperature inside the soil sample.

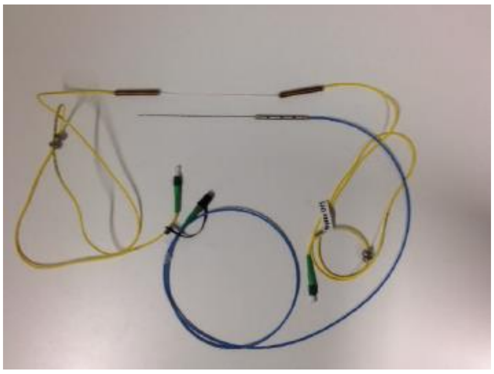

Figure 1. FBG thermistor string with blue plastic housing of the fiber and strain sensor with yellow plastic housing of the fiber.

We prepared and pre-frozen two clay samples 50×35×13 cm saturated with fresh and salt-water (34 ppt), respectively. The basic physical properties of the clay (gray-green color) are given in Table 1.

Table 1. The basic physical properties of the clay

Moisture content, %			Plasticity index Pl, %	Consistency index Cl, %	Density, g/cm3			Porosity, e	Water holding capacity, Wct
Moisture, W	Limits (GOST)				Particles, ρs	Soil, ρ	Dry soil, ρd		
	Liquid, Wl	Plastic, Wp							
35.0	37.4	19.1	18.3	0.87	2.67	1.82	1.35	0.978	0.366
Data file No.	Size of particles, mm								
	Composition of grains, %								
	1-0.5	0.5-0.25	0.25-0.1	0.1-0.05	0.05-0.01	0.01-0.005	0.005-0.002	<0.002	1-0.5
0.96	–	0.3	6.1	8.5	21.2	14.5	11.1	<0.003	0.96

One not through cut (0.8×10×7 cm) was made in the center of each sample for subsequent investigation of the water penetration and water freezing effects on the clay deformations. FBG temperature string and FBG strain sensors were used to measure soil temperature and deformations. Strain sensors were mounted on the surface of soil samples with brackets and screws, temperature strings were placed in drilling holes with diameter of 2 mm. Temperature probes Testo-176 were placed in the cuts to measure water-ice temperature. Soil samples with installed measurement systems is shown in Fig. 2. Similar FBG sensors were installed on the samples of fresh and sea ice in the same room. The sea ice salinity was 4 ppt.

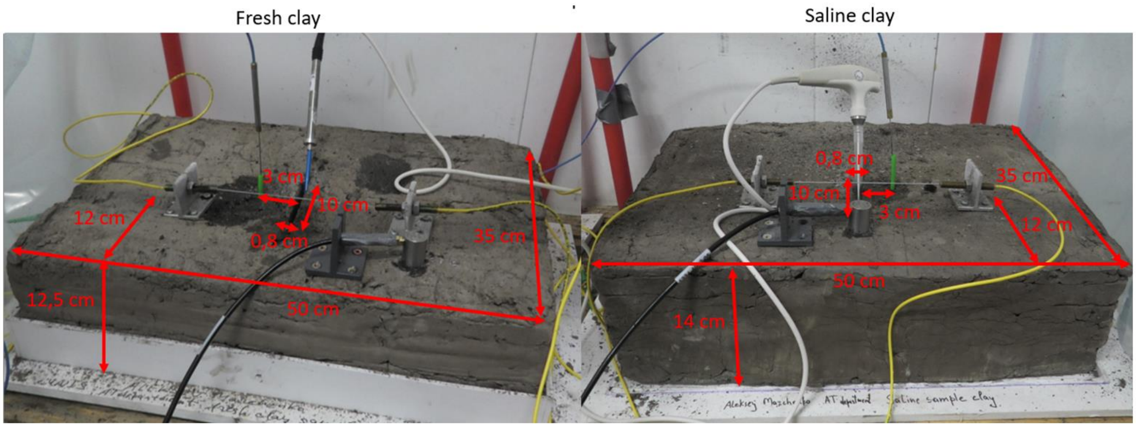

Figure 2. Clay samples and measurement installation.

RESULTS

Figure 3 shows the dependencies of the mean temperature in the soil and sea ice sample versus time. The dependence of the air temperature near the soil surface is shown in the same figure. The air temperature amplitude was about 10°C in the air. The ice temperature amplitude was smaller on 1°C. The amplitude of the fresh soil temperature was about 6ºC, and the amplitude of the saline soil temperature was only 4°C. It means that the specific temperature conductivity of the soils is smaller the sea ice conductivity. It is probably related with larger amount of unfrozen water in the soil samples in comparison with amount of liquid brine in sea ice.

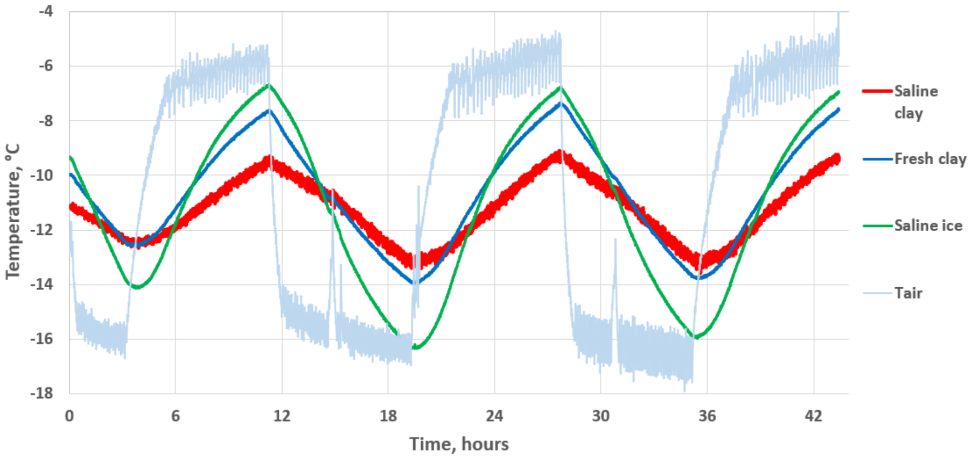

Figure 3. The mean temperatures of the ice and soil samples and the air temperature versus the time

Measured strains of the ice and clay samples are shown in Fig. 4 versus the time. At the beginning of the deformation curve and at each subsequent temperature switching rapid jumps of strains were observed in the soil samples. It is explained by softening of soil skeleton due to uneven crystallization of pore moisture leading to the appearance of local micro-stresses and microcracks (Votyakov, 1975). With a further increase in temperature, the acquired decompaction of the soil structure is preserved. This effect was not observed in the ice samples. Maximal strain amplitudes were observed in the fresh ice sample. The strain amplitude in sea ice sample were smaller, and the strain amplitudes in fresh and saline soils samples were similar and smaller than in sea ice sample.

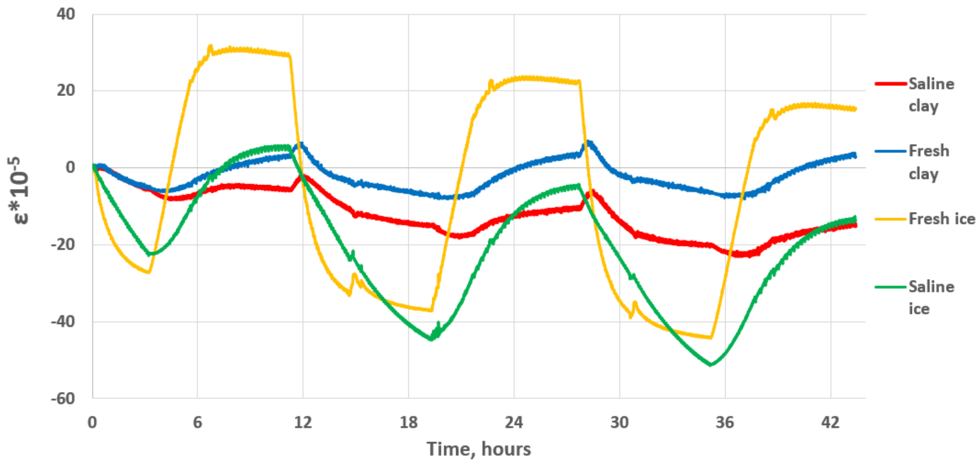

Figure 4. Strains measured in the ice and soil samples versus the time.

The dependence of strains in the soil samples and sea ice from their mean temperature was shown on the Figure 5. The mean temperature was calculated as the mean value of 10 temperature values measured by FBG temperature string at different depths in the soil. The hysteresis loops are well visible in the samples of saline soil and sea ice, and it is very thin in the fresh soil sample. The mean slope of the strain-temperature curves shown in Fig. 5 equals to the mean value of the linear coefficient of thermal expansion (CTE). Based on Fig. 5 the following values of CTE for saline soil, fresh soil and sea ice were calculated: CTEss = 0.8·10-5 K^{-1}, CTEfs = 1.6·10-5 K^{-1}, CTEsi = 5.6·10-5 K^{-1}. Herewith, studies of the CTE of frozen soils show that the deformability of the tested frozen soils does not directly depend on their mineral composition (salinity), but through values of the moisture content, porosity and structural features (Brushkov, 1998). Frozen soils are characterized by abnormally high CTE up to 2·10-3 K^{-1} and more (for clays), while for the mineral skeleton of the soil CTE = (0.4-8.0)·10-6 K^{-1} (Volokhov, Nikitin, Lavrov, 2017).

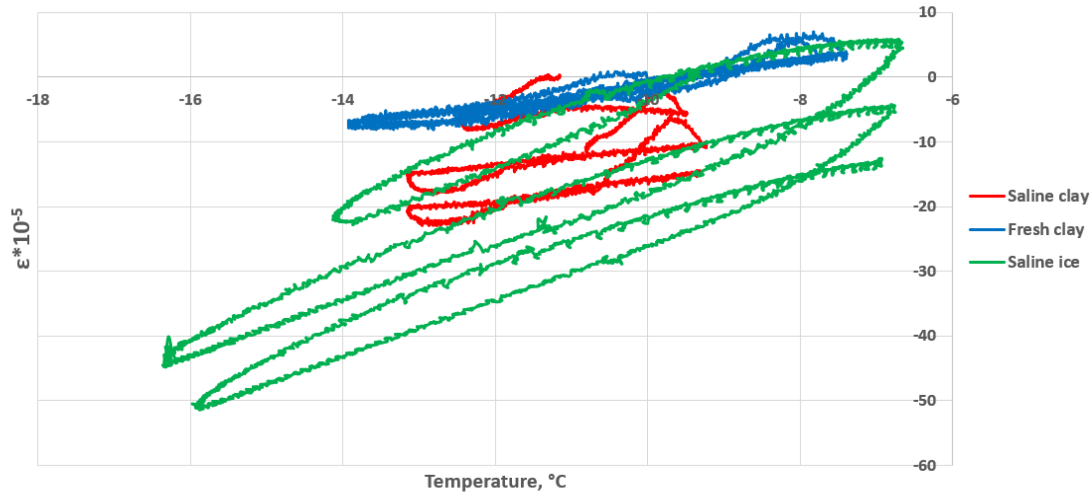

Figure 5. Dependences between average temperature inside sample and deformation.

Further, the temporal evolutions of the strain (red line) and temperature inside saline soil sample were observed (after sea water (salinity is 34 ppt) was added in the cut). The added water was at the freezing point (~ -1.9ºC). The air temperature near the soil surface (gray line Tair) and water/ice temperature inside the cut (green line Temp inside hole) are also shown in Fig. 6. The air temperature near the soil surface was around -9ºC during the experiment. Significant part of the sea water was frozen inside the cut probably during several minutes, and after that only liquid brine with high salinity left inside the soil. The moment when sea water was added in the cut coincides with sharp increase of the temperature inside the cut. The temperature stabilization inside the hole occurred in 1.5 hours. The soil temperature returned to the initial temperature after 2.5 hours. The strain response in tension extended over 6 hours. Maximal tensile strain accounted from the moment when the water was added in the cut reached $6 \cdot 10^{-5}$.

Also, the same temporal evolutions of the strain were determined in fresh soil sample (Figure 7). The air temperature near the soil surface (light blue line T_{air}) and water/ice temperature inside the cut (green line Temp inside hole) are also shown in Fig. 7. The air temperature near the soil surface was around -9ºC during the experiment. The fresh water was frozen inside the cut probably during several minutes or faster. This moment coincides with sharp increase of the temperature inside the cut. The temperature stabilization inside the hole occurred in 1.5 hours. The soil temperature returned to the initial temperature after 2.5 hours. The strain response in tension extended over 2 h. Maximal tensile strain accounted from the moment when the water was added in the cut reached $4 \cdot 10^{-5}$.

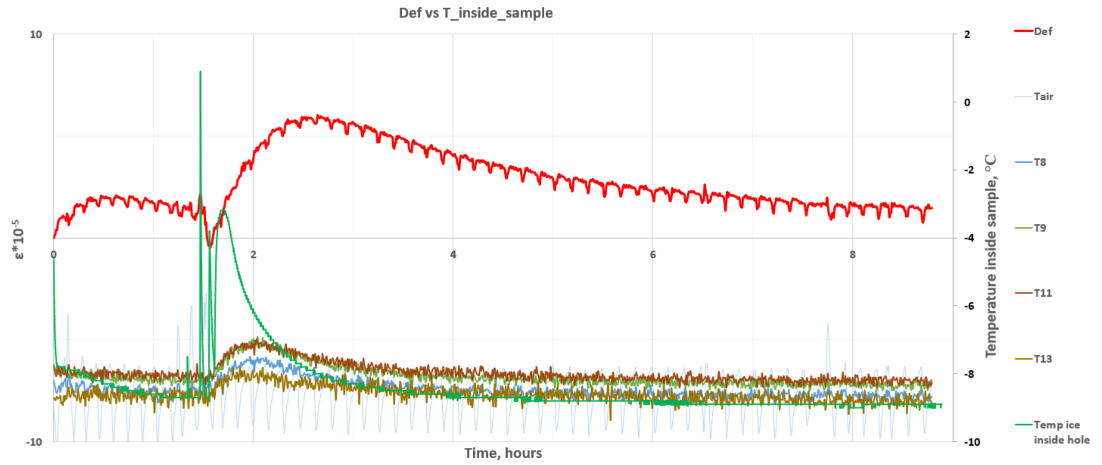

Figure 6. Water penetration effect on saline clay sample.

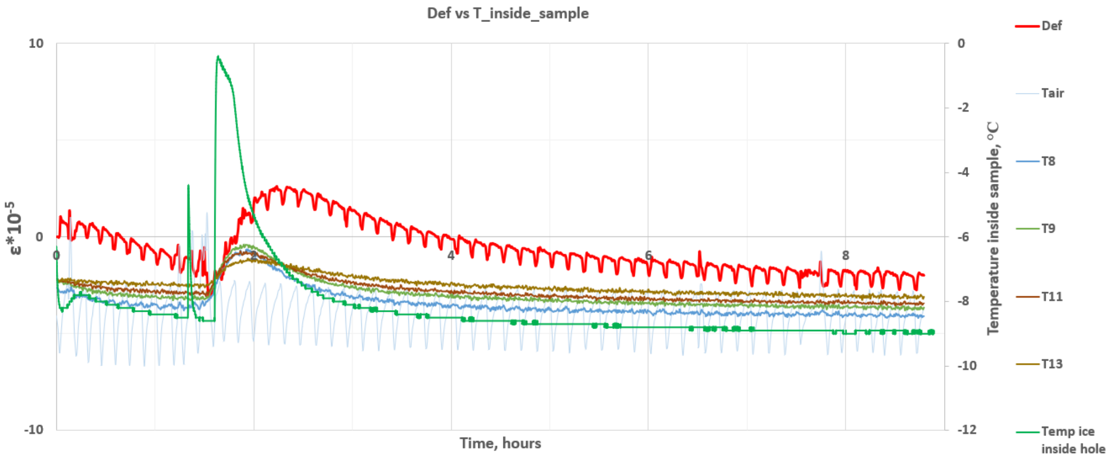

Figure 7. Water penetration effect on fresh clay sample.

DISCUSSION AND CONCLUSIONS

Cyclic change of the air temperature in the range from -5ºC to -20ºC with 12 h period influenced cyclic deformations of the saline soil and fresh soil samples, and sea ice sample placed in the same room. Deformations were caused by thermal expansion. Maximal strain amplitudes were registered in sea ice. The strain amplitudes in the fresh soil sample were approximately in two times greater the strain amplitudes in the saline soil sample. The mean values of the linear coefficients of thermal expansion of saline soil, fresh soil and sea ice, fresh were CTEss=0.8·10-5 K^{-1}, CTEfs=1.6·10-5 K^{-1}, CTEsi=5.6·10-5 K^{-1}. The hysteresis loops were greater in the saline soil and sea ice samples. Strain rates of tensile and compressive deformations accompanying respectively the temperature increase and decrease were not similar in the considered temperature range. Difference of the temperature and the thermally induced strains in the samples is explained by the difference in their thermodynamic characteristics including the specific heat capacity and the thermal conductivity. Probably the specific heat capacity of the saline soil sample was highest because of the liquid brine content. Temperature changes were associated with phase transformations in the soil and, as a result, temperature variations were smallest in the saline soil sample. Respectively, the thermal expansion was also smallest in this sample.

Freezing of water inside the cuts made in the saline soil and fresh soil samples influences tensile deformations. Temporal response on the fast filling of the cuts by sea water at the freezing point in the saline soil sample and fresh water at the freezing point in the fresh soil sample consists of the temperature increase and extension. Representative time of the response was greater in the saline soil sample. Tensile strains were also greater in saline soil sample. Since the air temperature was constant (-9ºC) during the experiments the soil heating is exlained by the latent heat release by the water freezing in the cuts. The latent heat released in the cuts volume and the heat flux propagated mainly in the soil, because the contact area of the cuts with the air was much smaller the contact area with the soil. Thermodynamic properties of the soils influenced temperature changes near the cuts, and it influenced in its turn the thermal expansion of the soil samples.

Various tools for modeling of complex thermal and hydrogeological processes are existing for the purpose of frozen soils studying which affect structures, including hydrotechnical facilities. Software systems using the finite element method (such as Plaxis 2D) allow to determine the stress-strain state of the foundation and select a structure that is applicable in the considering conditions. The results of this paper, the found and specified parameters of frozen soil can be used in such calculations for the goals of the necessary analysis at the design of hydrotechnical structures in the Arctic.

ACKNOWLEDGEMENTS

The team of authors expresses great appreciation to the project – Safety of Industrial Development and Transportation Routes in the Arctic, 2015–2019 (SITRA), with the financial support of which it became possible to conduct these studies.

REFERENCES

Alhimenko A.I., Belyaev N.D., Fomin Yu.N., 2003. *Safety of marine hydrotechnical structures*. - SPb: Lan. p.288.

Andersland O. B. and Ladanyi B., 2003. *Frozen Ground Engineering*. - p. 384

Brushkov A.V., 1998. *Saline frozen soils of the Arctic coast, their origin and properties.* M.: Moscow State University. - p.330.

Cheverev V.G., 2004. *Nature of cryogenic soils*. Moscow: Nauchnui Mir., p. 234 (in Russian).

Chzhan R.V., Velikin S.A., 2014. Safety of small and medium dams in permafrost regions. *Sciences in Cold and Arid Regions, 6(4)*, pp.331–339.

Ershov E.D., 1990. *Geocryology*. Moscow: Nedra, pp.559 (in Russian).

Grechishchev S.E., et al., 1983. *New methods of studying the composition, structure and properties of frozen soils*. "Nedra", Moscow (in Russian).

Marchenko AV, Lishman B, Wrangborg D, et al., 2016. Thermal Expansion Measurements in Fresh and Saline Ice Using Fiber Optic Strain Gauges and Multipoint Temperature Sensors Based on Bragg Gratings. *Hindawi Publishing Corporation. Journal of Sensors*, p.13.

Marchenko A.V., Nesterov A.A., Vasiliev N.K., et. al., 2020. Temperature Deformations of Soil Influencing Transportation Continuity in the Arctic Region. *Transportation Soil Engineering in Cold Regions, Volume 1, Lecture Notes in Civil Engineering 49*, pp.25-34

Nesterov A.A., Marchenko A.V., Vasiliev N.K., 2020. Thermal Deformations of Frozen Clay Caused by Cyclic Changes of Temperature and Thermal Impacts. Proceedings of the *25th IAHR International Symposium on Ice*

Volokhov S.S., Nikitin I.N., Lavrov D.S., 2017. Temperature deformations of frozen soils caused by rapid changes in temperature. *Moscow University Geology Bulletin – Vol. 72, no. 3*, pp.224–229.

Votyakov I.N., 1975. *Physical and mechanical properties of frozen and thawed soils of Yakutia*. Novosibirsk: Nauka. p.176 (in Russian).